Effect of ezrin regulation by sperm-borne miR-183 on the formation of microvilli and early development of bovine embryos.

Zhenzi Zuo
College of Veterinary Medicine, Northwest A & F University
Xu Liu
College of Veterinary Medicine, Northwest A & F University
Zheng Wang
College of Veterinary Medicine, Northwest A & F University
Fang Qiao
College of Veterinary Medicine, Northwest A & F University
Jingyi Wang
College of veterinary and Medicine, Northwest A & F University
Jingcheng Zhang
College of Veterinary and Medicine, Northwest A & F Universuty
Yong Zhang
College of Veterinary and Medicine, Northwest A & F University
Suzhu Qing
College of Veterinary and Medicine, Northwest A & F University
Yongsheng Wang (wangyongsheng01@nwsuaf.edu.cn)
Northwest Agriculture and Forestry University https://orcid.org/0000-0002-8301-4031

Research

Keywords: miRNA-183, ezrin, early embryonic development, microvilli, bovine

Posted Date: August 17th, 2020

DOI: https://doi.org/10.21203/rs.3.rs-53406/v1

Abstract

Background: Mature sperm contain both coding and non-coding RNAs, which can be delivered into an oocyte with the sperm at fertilization. Accumulating evidence shows that these sperm-borne RNAs play crucial roles in epigenetic reprogramming, remodeling, embryonic development, and offspring phenotype. MiR-183 is highly expressed in bovine sperm, and can be delivered into oocytes during fertilization.

Results: Here we used bioinformatics and luciferase assays to show that the ezrin gene, *EZR*, is one of the targets of miR-183 in early embryos, while gain- and loss-of-function studies demonstrated their regulatory relationship. Scanning electron microscopy showed that the density of microvilli on the surface of somatic cell nuclear transfer (SCNT) embryos was significantly higher than on *in vitro* fertilized (IVF) embryos and was significantly reduced by injection of miR-183. *EZR*-siRNA injected into SCNT embryos had a similar effect. This indicated that a deficiency in sperm-borne miRNA-183 might lead to abnormal changes in microvilli by down-regulating ezrin protein. We used bioinformatics to select the proteins that worked in combination with ezrin to regulate microvilli function. Co-IP mass spectrometry and immunofluorescence identified SLC9A3R1 as the protein functioning in synergy with ezrin in early bovine embryos. Gain-of-function studies showed that miR-183 significantly improved developmental competence of SCNT embryo in terms of cleavage (76.63% vs 64.32%, $p<0.05$), blastocyst formation (43.75% vs 28.26%, $p<0.05$), apoptotic index (5.21% vs 12.64%, $p<0.05$), and the trophoblast ratio (32.65% vs 25.58%, $p<0.05$) in day 7 blastocysts.

Conclusions: In conclusion, the present studies indicated that sperm-borne miR-183 might influence the formation of microvilli and embryo development by regulating expression of *EZR* mRNA.

Background

Mammalian embryonic development begins with the penetration of a sperm into an oocyte [1]. Previously, it was thought that only oocytes contained regulators of embryonic development. However, a large body of evidence suggests that sperm also contains significant amounts of proteins, mRNAs, tRNAs, tsRNAs, PIWI-interacting RNAs, and miRNAs, which have recently been shown to have important effects on embryonic development [2, 3, 4, 5]. Many post-transcriptional regulatory factors, such as miRNAs, can be delivered into oocytes during fertilization. These play crucial negative regulatory roles in gene expression and coordinate with the positive regulatory activity of embryo-specific protein regulatory factors to form a system for precise regulation of expression [6]. Although miRNAs account for only one to three percent of vertebrate genomes, they target nearly thirty percent of genes [7]. Because miRNA sequences are homologous, a single miRNA can effectively regulate hundreds or thousands of target genes, while a single target gene can be regulated by multiple miRNAs at the same time [8]. SCNT is a technique that can complete the embryonic development without the need for paternal genetic material, which provides a convenient condition for studying sperm-borne miRNAs. In a previous investigation, we extracted small RNAs from sperm, injected them into bovine SCNT embryos, and discovered that these sperm-borne small RNAs were crucial for regulating early embryonic development in terms of first cleavage, reprogramming,

and embryonic developmental competence [9]. Identifying sperm-borne small RNAs and determining their roles in fertilization and embryonic development might improve our understanding of embryogenesis. We had established a bovine sperm miRNA library through high-throughput sequencing and found that miR-183 was highly expressed in sperm [3]. Evidence indicated that miR-183 was an important tumor suppressor that controlled the migration and invasion of osteosarcoma cells by reducing ezrin expression [10-12]; however, there were few reports on the role of miR-183 in early embryonic development.

Ezrin is an 82 kDa phosphorylated cytoskeletal protein [13]. In mammals, ezrin together with radixin and moesin, form the ERM family. The ERM complex is a key regulator of microvilli formation and is expressed in many types of cells [14]. Several studies have shown that ERM proteins play a significant role in the formation and extension of microvilli by connecting membrane proteins to the actin cytoskeleton. In cells deficient in ezrin, the number of microvilli are significantly decreased [15]. Ezrin plays an important role in the establishment of polarity, the development of the actin terminal network, and villi morphology in intestinal epithelial cells [16]. Several studies have found that ezrin was involved in the formation of microvilli on mouse oocytes after maturation, fertilization and preimplantation of the embryo [17]; but little work has been done on ezrin's function in embryonic development and the mechanism of its regulation.

Although there is no known model of microvillus formation, it has been hypothesized that ezrin can locally recruit proteins which are needed for cytoskeletal or membrane remodeling, such as EBP50 [18]. EBP50 (Na^+/H^+ exchanger regulatory factor 1, NHERF1), SLC9A3R1, and the PDZ protein regulate planar cell polarity and motile cilia organization. The FERM domain of ezrin and the ERM domain of SLC9A3R1 can dynamically bind to microvilli and regulate their development. This interaction may be involved in the formation of ion channels on the surface of the microvilli, which is related to material exchange, and optical and acoustic induction functions [19, 20]. Recent studies indicated that ezrin and SLC9A3R1 showed distinct interactions in the formation of cellular microvilli [21]. Most studies of the function and formation of microvilli have focused on various somatic cells and oocytes, however, much less is known about their formation and function in fertilization and embryonic development.

In the present study, the effects of sperm-borne miR-183 on microvilli formation and developmental competence of early embryos were investigated. In addition, the regulatory mechanism for microvilli formation in early embryos was elucidated as a prelude to exploring the role of paternal regulatory factors on embryonic development and microvilli formation in early embryos.

Materials And Methods

Oocyte collection and in vitro maturation (IVM)

Bovine oocyte collection and IVM were carried out as described previously [22]. The cumulus-oocyte complexes (COCs) were removed from 2-8 mm follicles (obtained from a slaughterhouse) under a stereo microscope (Nikon Ti-E, Japan), and washed three times with phosphate buffered saline (PBS) with 5%

fetal bovine serum (FBS). COCs with even cytoplasm and at least a three-layer cumulus were selected for IVM. The culture medium for IVM was TCM-199 bicarbonate buffer with 10% FBS, 1 μg/mL 17ß-estradiol, and 0.075 IU/mL human menopausal gonadotropin (TCM-199, Gibco, BRL, Grand Island, NY, USA). Groups of 300 COCs were cultured in 4 mL medium in humidified air with 7% O_2, 5% CO_2 at 38.5°C for about 20 h. The cumulus cells outside the zona pellucida of the oocytes were removed with 0.1% hyaluronidase, and oocytes exhibiting the first polar body (Pb) were selected for subsequent experiments.

In vitro fertilization (IVF)

IVF were carried out as previously described [23]. Briefly, frozen semen (Yang Ling Ke Yuan Co. LTD, China) was thawed at 37°C, placed in a 15 mL tube with 5 mL Brackett and Oliphant (BO) medium supplemented with 20 μg/mL heparin and 6 mg/mL BSA, and incubated for 30 min at 38.5°C under 7% O_2, 5% CO_2. The treated semen supernatant was transferred to a 1.5 mL tube, centrifuged at 1200 g for 5 min and the sperm pellets recovered. The sperms were diluted to 2×10^6 sperm/mL, and 40 μl aliquots were added to 20-25 matured COCs in a volume of 460 μl BO-IVF medium (IVF Bioscience, Falmouth, United Kingdom). After IVF for 20 h, cumulus cells and excess sperm were removed from the oocytes by incubation in PBS containing 0.1% bovine testicular hyaluronidase. The oocytes with a second Pb were selected for further culture.

Somatic cell nuclear transfer (SCNT)

The procedures for SCNT were carried out as previously described [24]. Briefly, after IVM, cumulus cells were separated from COCs by incubation with 0.1% bovine testicular hyaluronidase in PBS. Metaphase II (MII) oocytes with first Pb were selected and stained with 10 μg/mL Hoechst 33342 for 10 min prior to micromanipulation. Enucleation was performed using a 20 μm glass pipette by aspirating the first Pb and a small amount of the surrounding cytoplasm in a 100 μL micro-drop of PBS supplemented with 10% FBS and 7.5 μg/mL cytochalasin B (CB). The extracted cytoplasm was examined under ultraviolet illumination in another micro-drop to confirm successful enucleation. The nuclear donor cells were ear fibroblasts from fetal Holstein cows that were serum-starved, and nuclei were injected into the perivitelline space of successfully enucleated oocytes. The oocyte-cell couplet was formed by electrofusion. Successfully reconstructed embryos were incubated in mSOFaa containing 5 μg/mL cytochalasin B for 2 h, activated with 5 μM ionomycin for 4 min, then with 1.9 mM dimethynopyridine for 4 h in mSOF. After activation, the embryos were cultured in 50 μL drops of mSOFaa medium supplemented with 8 mg/mL BSA under a humidified atmosphere of 7% O_2, 5% CO_2 at 38.5°C. The cleavage rate was determined at 48 h after culture, and blastocyst formation was counted on day 7 of culture.

Microinjection

The concentration of double-stranded miR-183 mimic / miR-183 mimic control for microinjection (Transgen, Beijing, China) was adjusted to 2 ng/μL as described previously [25]. Double-stranded RNA is necessary to increase stability during the experimental procedure and to facilitate the formation of the miRISC in cells. *EZR*-siRNA, *EZR*-siRNA control, *Slc9a3r1*-siRNA and *Slc9a3r1*-siRNA control were

produced by GenePharma (Shanghai, China). About 2 μL of injection solution was loaded into a microinjection needle (Eppendorf, Hamburg, Germany). The embryos for injection were transferred into PVA micro-droplets and covered with mineral oil. Changes in the cytoplasm were monitored during injection to ensure that the pulse pressure and injection volume of the experimental group and the control group were as consistent as possible. Injected embryos were then transferred into pre-balanced mSOF medium and cultured at 38.5°C in an atmosphere of 7% O_2, 5% CO_2.

Dual luciferase reporter gene assay

For the testing of target genes using TargetScan, PicTar, miRanda websites and the relevant literature (Supplementary data 7), *EZR* (ezrin gene), *Pdcd6* and *Ppp2ca* were selected as candidate targets of miR-183 after KEGG pathway analysis (Supp. Data 8). For the target gene test, the 3'-UTR regions of the target genes were amplified using fetal bovine liver tissue as cDNA template. The primer sequences are given in Table 1 and Table 2. Each 50 μL PCR reaction contained DNA polymerase (TransStart FastPfu, Beijing, China), 1 μL; 5×buffer (TransStart FastPfu, Beijing, China), 10 μL; forward primer (10 mM), 1 μL; reverse primer (10 mM), 1 μL; dNTPs (10 mM), 4 μL; template, 1 μg; dd H_2O, 35 μL. The PCR reaction procedure was as follows: 94°C for 3 min; (94°C for 30 s, 60°C for 30 s, 72°C for 30 s) 40 cycles; 72°C for 10 min, 16°C for 10 min. The sequence and pSicheck-2 carrier involved a dual enzyme reaction with restriction endonucleases *Not*I and *Xho*I, followed by ligation. Afterwards, the target gene reporter carriers were constructed: psi-*EZR*, psi-*Pdcd6*, psi-*Nck2*, psi-*Ppp2a*, psi-*Crk*, psi-*Teme150a*, psi-*Srek1ipi*, psi-*Map3k4*, psi-*Slc35a1*. With the target gene reporter carriers as templates, the target gene psi-mutants, psi-mut-*EZR*, psi-mut-*Pdcd6* and psi-mut-*Ppp2a*, were successfully constructed.

The dual luciferase reporter assay was performed using a TransDetect double-luciferase reporter assay kit (TransGen Biotech, China) following the manufacturer's procedure. Briefly, Renilla luciferase substrate and firefly luciferase substrate were thawed at 16°C. Cells in 24-well plates were washed three times with pre-cooled saline, mixed with 100 μL of lysis buffer and allowed to lyse for 15 min at room temperature. Lysates were centrifuged at 12,000 g for 10 min at 4°C, supernatants were mixed with firefly luciferase substrate, and 20 μL aliquots were added to each well of a 96-well plate. Fluorescence values of the firefly luciferase reporter gene were measured with a chemiluminescence apparatus, with three well repeats for each sample. Afterwards, the Renilla luciferase substrate was added, and the fluorescence values of the Renilla luciferase reporter gene were detected with the chemiluminescence instrument.

Immunofluorescence staining of embryos

The embryos were washed three times with PBS containing 0.2% PVA (PBS/PVA) and fixed overnight in 4% paraformaldehyde at 4°C. After washing with PBS/PVA three times, five mins each time, they were transferred into PBS/PVA containing 0.1% Triton X-100 for permeabilization, 30 min at 25°C. After washing, the embryos were kept in blocking buffer (Beyotime P0102, Shanghai, China) for three hours at room temperature. After washing, the embryos were incubated with the primary antibody (Abcam, Cambridge, UK) overnight at 4°C. After washing, they were incubated with secondary antibody (Beyotime,

Shanghai, China) at room temperature in the dark for 2 h. The DNA was stained with 4, 6-diamidino-2-phenylindole (DAPI), (Beyotime C1005, Shanghai, China) for 3-5min. Finally, the embryos were placed on glass slides and examined using a Nikon Eclipse Ti-S microscope equipped with a 198 Nikon DS-Ri1 digital camera (Nikon, Tokyo, Japan).

The Dead End TM colorimetric TUNEL system (Promega, Madison, WI, U.S.) was used to detect blastocyst apoptosis. The blastocysts were fixed overnight in 4% paraformaldehyde at 4°C, permeabilized in 0.1% Triton X-100 for 30 min at 25°C, transferred into E buffer micro-droplets at room temperature for 5 min, and incubated with FITC-conjugated dUTP and terminal deoxynucleotidyl transferase at 37°C for 1 h in the dark. 2×SSC (SSC: 0.15 mol/L sodium chloride and 0.015 mol/L sodium citrate) was added to stop the reaction and samples were allowed to stand for 15 min. Samples were stained with DAPI at room temperature in the dark for 8 min. Staining was observed under a fluorescence microscope (Nikon, Tokyo, Japan).

Reverse transcription and qRT-PCR

Total RNA was isolated from about 10 SCNT embryos for each experiment. RNA reverse transcription was performed using the miScript II RT kit according to the manufacturer's directions (Qiagen, Germany). Briefly, we mixed 2 μL of 10×miScript Nucleics mix, 4 μL 5×miScript Hispec buffer, 10 μL purified RNA, 2 μL miScript reverse transcriptase mix and 2 μL RNase-free water for each 20 μL reaction. Thermocycling conditions were as follows: 37°C for 60 min and 95°C for 5 min. Primer sequences are listed in Table 3. The reverse transcription process was performed according to the instructions for the TransScript first-strand cDNA synthesis super-mix (Transgen, Beijing, China). The procedure was as follows: 25°C, 10 min; 42°C, 30 min; 85°C, 5 min. Quantitative RT-PCR was performed according to the procedure for the SYBR premix Ex Taq (Perfect Real-Time), and the primers were synthesized at Xi 'an Qing Ke. The PCR procedure is as follows: 95°C, 30 s; (95°C 5s, 60°C 30 s, 95°C 15 s) 35 cycles; 60°C, 5 min. The $2^{-\triangle\triangle Ct}$ method was used to calculate the relative expression level of the target mRNAs and statistical comparisons were conducted by one-way ANOVA.

Protein identification by western immunoblot

Aliquots of protein extracts were run at a constant voltage of 80V on an SDS-PAGE gel until the samples entered the separating gel, at which time it was switched to a constant voltage of 120 V. The gel containing the target proteins and size markers was blotted to PVDF film for 120 min at a constant current of 250 mA and 4°C with blocking buffer, overnight at 4°C. The first antibody was diluted and the blot was incubated at 4°C for 12 h. After washing twice with 1×TBST, the second antibody was diluted and incubated with the blot at room temperature for 2 h in the dark.

Co-IP

Primer 5 software was used to analyze and synthesize the upstream and downstream primer sequences of pCMV-HA-*Slc9a3r1* and pCMV-EGFP-*EZR* vectors (Supp. Data 9). PCR amplification was performed as

described in Section 2.5. The reaction conditions were as follows 95°C for 5 min, (95°C for 30 s, 56°C for 30 s, 72°C for 2 min) 30 cycles, 72°C for 10 min. The amplified DNAs were run on agarose gels, the bands were cut out and the DNAs were extracted (OXOID, UK). Restriction endonucleases, *Nhe*I (GCTAGC) and *Age*I (ACCGGT) were used to perform a double digest of the PCR-amplified product and the pCMV-EGFP skeleton vector, respectively. At the same time, *Bgl*II (AGATCT) and *Not*I (GCGGCCGC) were used for double digestion of the PCR amplified product and the pCMV-HA skeleton carrier, respectively. The reaction conditions were as follows: 100×BSA, 0.5 μL; 10×NEB buffer, 5 μL; DNA, 5 μg; enzyme A, 0.5 μL; enzyme B, 0.5 μL; dd water to 50 μL, incubate at 37°C for 8 h. The ligation was performed with a DNA ligation kit: dd H_2O, 4 μL; linearized vector, 1 μl (45-150 ng); cDNA, 1 μl (45-100 ng), Quick-Clone mix, 4 μL. The reconstructed carrier was used for transfection, and identified by enzyme digestion (*Kpn*I-*Xho*I was used for double digestion of pCMV-EGFP-*EZR*, and *Bgl*II-*Not*I was used for double digestion of pCMV-HA-*Slc9a3r1*) (Promega, USA) and PCR, the forward primer and reverse primer sequences of pCMV-HA-*Slc9a3r1* and pCMV-EGFP-*EZR* plasmid carrier were designed, and the primer sequences are given in Supp. Data 10. The PCR reaction procedure was as follows: 10×TransStart Taq buffer, 2 μL; Trans Fast Taq DNA polymerase, 0.2 μL; P1 (universal primer), 0.4 μL; P2 (universal primer), 0.4 μL; dNTPs (10 mM), 0.4 μL; take a small amount of bacterial colony on a micropipette tip as template; dd H_2O, 16.6 μL. 95°C for 5 min, (95°C for 30 s, 56°C for 30 s, 72°C for 2 min) 30 cycles, 72°C for 10 min. After successful sequencing, endotoxin-free plasmid extraction was carried out (Promega, USA). The three combinations of ezrin-GFP & HA-empty, GFP-empty & HA-SLC9A3R1 and ezrin-GFP & HA-SLC9A3R1 were transfected into 293T cells using Lipofectamine 2000 (Invitrogen, USA). Total protein was extracted from each group by incubating in a boiling water bath for 5 min, an ice bath for 2 min, and centrifugation for 2 min at 20,000 g, followed by SDS-PAGE electrophoresis. Ezrin-GFP & HA-SLC9A3R1 protein were extracted and mixed with 10 μL anti-HA-tag magnetic beads, and the other group was mixed with 10 μL anti-GFP-tag magnetic beads. After reversing and mixing to balance the beads, they were centrifuged at 5,000 g for 15-30 s at 4°C and supernatants were removed. The supernatants were mixed with 10 μL anti-HA-tag magnetic beads (another group of protein supernatants were mixed with 10 μL anti-GFP-tag magnetic beads), mixed evenly, and incubated at 4°C for 3 h. Centrifugation was performed at 5,000 g, 4°C for 30 s and supernatants were removed. Pellets were washed four times with 1 mL aliquots of wash buffer, 5 min each time. The pellets containing immunoprecipitated proteins were resuspended in 35 μL SDS loading buffer, placed in a boiling water bath for 5 min, then on ice for 2 min, followed by centrifugation for 2 min at 20,000, and running on an SDS-PAGE gel.

Preparation of embryo samples for scanning electron microscopy

Embryo samples from each group were collected and fixed in 2.5% glutaraldehyde at 4°C overnight. Before dehydration, the embryo samples were washed four times, 10 min each, with 1M PBS, pH 7.2. Fixed/washed embryo samples were successively placed in 30%, 50%, 70%, 80% and 90% ethanol for 15 min each time, then dehydrated in 100% ethanol three times, 30 mins each time. After critical-point drying and metal spraying, the microstructure of the embryo microvilli was observed under a scanning electron microscope (Leica TCS SP8, Germany).

Statistical analysis

Data were averaged from at least three independent experiments. Three technical replicates were applied for RT-qPCR to detect the expression in the different groups. The comparative threshold cycle method ($2^{-\triangle\triangle Ct}$) was used to calculate the relative expression of miRNAs. Statistical comparisons were conducted by one-way ANOVA. Immunofluorescence intensity was determined with Image J software (National Institutes of Health, Bethesda, MD, USA). Mean gray value (Mean) = integrated density (IntDen) / area. Statistical analyses were conducted using the SPSS software package (SPSS Inc, Chicago, IL, USA). Data were expressed as means ± standard errors of the mean (SEM), and $p < 0.05$ was considered statistically significant.

Results

Screening for target genes of miR-183

The expression level of bta-miR-183 in oocytes, PN (pronucleus), 2-cell and 4-cell stages of IVF embryos was first determined. As shown in Supp. Data 1, miR-183 expression was lower in MII oocytes, increased sharply in 1-cell zygotes after fertilization, then continuously decreased from the 2-cell to the 4-cell stage. These results suggested that sperm-borne miR-183 might be active from fertilization to the 2-cell stage.

According to predictions of target genes using TargetScan, PicTar and miRanda software and the relevant literature [26], *EZR*, *Pdcd6* and *Ppp2ca* were selected as candidate targets of miR-183 (Supp. Data 2). The levels of firefly luciferase and Renilla luciferase of candidate genes was measured after the miR-183 mimic, negative mimic control and recombinant plasmid pSicheck-2-3'UTR were co-transfected into 293T cells. As shown in Figure 1A, the luciferase activity of *EZR*, *Pdcd6* and *Ppp2ca* was less in the wild-type group, while that of the mutant group remained unchanged, indicating that the 3'-UTR region of these three target genes was regulated by miR-183. After transfection of fetal bovine fibroblast cells with miR-183 mimic/control group, RNA was extracted after 36 h, reverse transcribed, and the expression of *EZR*, *Pdcd6* and *Ppp2ca* was quantitated by qRT-PCR. After transfection with miR-183 mimic, the levels of *EZR*, *Pdcd6*, and *Ppp2ca* mRNA were down-regulated relative to the control group (**Fig. 1B**). After transfection of fetal bovine fibroblasts with miR-183 mimic/control or miR-183 inhibitor, total protein was collected at 48 h for western blot. After transfection of fibroblasts with miR-183 mimic, ezrin protein expression was significantly decreased (**Fig. 1C**). After transfection with miR-183 inhibitor, ezrin protein level increased, while expression of the internal reference GAPDH protein remained unchanged.

The expression of *EZR* in SCNT embryos during the 2-cell and 4-cell stages was significantly higher than that in the IVF group (Supp. Data 3). Expression of the target gene *Pdcd6* in SCNT embryos was significantly higher in the 1-cell, 2-cell and 4-cell stages than that in the IVF group. The expression of the target gene *Ppp2ca* in SCNT embryos was significantly higher in the 4-cell stage than in the IVF group. After microinjection of miR-183-inhibitor, the expression levels of *EZR*, *Ppp2ca* and *Pdcd6* in MII oocytes, PN, 2-cell and 4-cell stages of IVF embryos were quantitatively detected and the mRNA levels of target

genes *EZR*, *Ppp2ca* and *Pdcd6* were increased to different degrees in PN, 2-cell and 4-cell, with no significant difference in pronucleus; but the mRNA levels of target genes were significantly increased in 2-cell and 4-cell embryos (**Fig. 1D**). Based on these results, *EZR* was selected as the target gene of miR-183 in early-stage bovine embryos.

Verification of the targeting relationship between miR-183 and its target gene, *EZR*

Ezrin expression was measured in MII oocytes, and PN, 2-cell, 4-cell IVF embryos by immunofluorescence staining. Ezrin was distributed between cytoplasm and cortical areas, but significantly enriched at cell contact points, mainly in cortical areas, especially at the 2-cell and 4-cell stages (**Fig. 2A**). After miR-183 inhibitor injection, ezrin protein was increased in the cytoplasm. The ezrin fluorescence intensity in both 2-cell and 4-cell stages of the miR-183 inhibitor group was higher than that in the control group, which was consistent with the results for quantitation of *EZR* mRNA in the early stage (**Fig. 2A, 1D**). However, the change of ezrin fluorescence intensity after injection was inconsistent with the quantitative results of *EZR* mRNA at the prokaryotic stage, suggesting that ezrin might be regulated by miR-183 post-transcriptionally during this stage. As shown in Figure 2C, the expression of parthenogenetic embryos after injection of the miR-183 mimic at PN, 2-cell and 4-cell stages was significantly lower than that of parthenogenetic miR-183 mimic control group ($p<0.05$). In addition, *EZR*-siRNA significantly reduced expression of the *EZR* gene (**Supp. Data 4**). Ezrin protein expression in parthenogenetic embryos during the PN, 2-cell and 4-cell stages was determined by immunofluorescence staining. The expression of *EZR*-siRNA in parthenogenetic embryos during PN, 2-cell and 4-cell was significantly lower than that in the parthenogenetic *EZR*-siRNA control group (**Fig. 2e**, $p<0.05$). After injection of miR-183 mimic and *EZR*-siRNA, ezrin protein expression in parthenogenetic bovine embryos was significantly lower than in the miR-183 control group and *EZR*-siRNA control group, which was closer to the ezrin protein expression level in IVF embryos (**Fig. 2G**).

Screening and validation of proteins interacting with ezrin

The expression trend of *Slc9a3r1* in PN, 2-cell and 4-cell was determined by qRT-PCR in parthenogenetic embryos. It was found that the expression in PN was significantly higher than that in the 2-cell and 4-cell embryos (**Supp. Data 5**, $p<0.01$). As shown in Figure 3A, the expression levels of ezrin protein and SLC9A3R1 protein were significantly higher in the miR-183 mimic control SCNT embryo group than in IVF embryos, while they were significantly decreased in the miR-183 mimic injection SCNT embryos group. Similarly, there was a significant difference in the expression of ezrin and SLC9A3R1 protein between the *EZR*-siRNA control group embryos and IVF embryos. The fluorescence intensity of ezrin and SLC9A3R1 protein in *EZR*-siRNA embryos was significantly decreased; thus, the expression of SLC9A3R1 protein could be influenced by ezrin. The constructed carriers of pCMV-HA-*Slc9a3r1* and pCMV-EGFP-*EZR* are shown in Supp. Data 6. Ezrin-GFP & HA-empty, GFP-empty & HA-SLC9A3R1, ezrin-GFP & HA-SLC9A3R1 were used in the experiment (**Fig. 3C**). In the ezrin-GFP & HA-SLC9A3R1 group, IP: GFP, IB: HA, the SLC9A3R1 band is visible. On the contrary, in the IP: HA, IB: GFP, the ezrin band is prominent. These results indicate that there was a natural interaction between ezrin and SLC9A3R1. InPut results were

taken as a positive control, and empty plasmid vector was taken as a negative control, indicating that there were no false positive results.

MiR-183 targets ezrin to regulate microvilli formation in early bovine embryos

The microvilli on the embryo surface were examined by scanning electron microscopy (**Fig. 4**). Under a magnification of 3000×, the surface of NT-miR-183 mimic control and NT-*EZR*-siRNA control embryos had a greater 'plush' appearance and longer microvilli than that of the IVF group, the miR-183 mimic injection group and the *EZR*-siRNA injection group. Under 50,000× magnification, it was observed that, compared to the NT-miR-183 mimic control group and NT-*EZR*-siRNA control group, the microvilli density on the embryo surface decreased in the IVF group, the miR-183 mimic injection group and the *EZR*-siRNA injection group; the leakage area increased and the abnormal increase of microvilli was reversed. Embryos from the SLC9A3R1 knock-down group showed a phenotype similar to that of the miR-183 and ezrin knock-down groups; microvilli on the surface of NT-*Slc9a3r1*-siRNA embryos were shorter and of lower density than those of the control group (**Fig. 4**). This result further confirmed that SLC9A3R1 interacted with ezrin to regulate the formation of embryonic microvilli after fertilization.

Effects of miR-183-ezrin on the developmental competence of bovine embryos

MiR-183 injection significantly improved the developmental competence of SCNT embryos in terms of cleavage rate (76.63% vs 64.32%, $p<0.05$) and blastocyst formation rate (43.75% vs 28.26%, $p<0.05$) when compared to control (**Fig. 5A-B**). Similarly, the cleavage rate (71.43% vs 63.27%) and the blastocyst formation rate (36.54% vs 27.27%) were significantly improved in the *EZR*-siRNA injection group over the control group ($p<0.05$).

As shown in Figure 5c, the apoptotic index in blastocysts from the NT-miR-183 mimic group was significantly lower than that of the NT-miR-183 mimic control group ($p<0.05$), and the apoptotic index in blastocysts from the NT-*EZR*-siRNA group was also significantly lower than the control group ($p<0.05$). Blastocysts from the IVF group had a significantly lower apoptotic index than the NT-miR-183 mimic control, the NT-miR-183 mimic, the NT-*EZR*-siRNA control and the NT-*EZR*-siRNA group ($p<0.01$). The percentage of trophoblastic cells in the NT-miR-183 mimic and the NT-*EZR*-siRNA injection group was significantly higher in day seven blastocysts than in the NT-miR-183 mimic control and the NT-*EZR*-siRNA injection group, indicating that the embryonic development quality was effectively improved (**Fig. 5E**). The percentage of trophoblastic cells in the IVF group on day seven was significantly higher than that in the SCNT group.

Discussion

Accumulating evidence has shown that sperm-borne non-genetic molecules play various roles in fertilization and embryonic development, such as oocyte activation [27], cleavage [28], epigenetic remodeling [29], and transgenerational inheritance [30]. Here, for the first time we observed a regulatory relationship between sperm-borne miR-183 and microvilli formation in early bovine embryos. To reveal

the underlying mechanism, the miR-183 target genes and interacting proteins were identified. This study expands our understanding of the activity of sperm in directing embryonic development.

Microvilli are part of a special structure on the surface of cells with fingerlike projections composed of microfilaments formed by the aggregation of actin. The number and diameter of microfilaments vary to meet different functional needs [19]. The increased surface area and movement of microvilli promote the absorption of substances, liquid transport, signal transmission and other processes [31, 32]. It is well known that the microvilli on the surface of the oocyte can encase the sperm during fertilization, which is conducive to efficient fertilization [33]. In the present study, we found that the microvilli on IVF embryos had a lower density, and were shorter and smaller than those of SCNT embryos. This abnormality in microvillus morphology might contribute to the low developmental competence of SCNT embryos, although the function of microvilli in embryonic development is unknown. We hypothesized that miR-183 targeting of the *EZR* gene could reduce the density and length of the microvilli on the embryonic surface. During fertilization, the oocyte microvilli wrap the sperm, which enhances egg penetration [33], but after fertilization, the density and length of the microvilli on the embryo surface decrease significantly. It has been reported that during embryo implantation, the microvilli on its surface have a greater density and length, which is more conducive to attachment and invasion of the endometrial epithelium [34, 35]. The low density and short length of microvilli on the surface of an early embryo may facilitate its migration from ampullary to uterus by preventing ectopic attachment. Ezrin and SLC9A3R1 interact to form ion channels on the surface of the microvilli, and their function is mainly related to material transport, optics, acoustics and induction [20]. The reduction in length and density of microvilli on early embryos may be a protective mechanism to reduce light and acoustic stress.

There have been many studies indicating that SLC9A3R1 and ezrin are precisely co-located in many types of epithelial microvilli [36], and their main function is to promote ion transport and absorption by cells [37]. The SLC9A3R1 protein has been shown to be important for organizing and maintaining ezrin's localization at the surface of cell membranes [38]. Ezrin and SLC9A3R1 are usually bound together [39] and localized to polarized epithelial cells [40, 41]. Ezrin is usually stable in cell membranes [40], but a lack of SLC9A3R1 can cause ezrin dissociation from the cytoskeleton [42]. The epithelial cells of mice deficient in SLC9A3R1 have short aberrant microvilli, similar to the phenotype of ezrin knockout mice, suggesting that these two proteins play a role in the regulation of microvillus structure [16, 38]. However, it is unknown whether the same function and interaction between SLC9A3R1 and ezrin occurs in bovine embryo microvilli formation. In the present study, we carried out a co-IP in 293T cells to determine if there was an interaction between SLC9A3R1 and ezrin in somatic cells as previously reported, and the result was consistent with previous observations [42]. Next, we knocked down SLC9A3R1 and ezrin in early embryos, and found that the two proteins had similar roles in the formation of microvilli. These studies indirectly demonstrated that SLC9A3R1 and ezrin might interact in the formation of embryonic microvilli.

Conclusion

In summary, the binding of ezrin to SLC9A3R1 is an important process in fertilization, and is accompanied by the dynamic regulation of ezrin expression by sperm-borne miR-183. Based on our current research results, we speculate that the dynamic changes in microvilli before and after fertilization might play crucial roles in the subsequent development of embryos.

Abbreviations

EZR:ezrin; SCNT:somatic cell nuclear transfer; IVF: in vitro fertilized; Co-IP: Co-Immunoprecipitation; ERM: Ezrin-Radixin-Moiesin; EBP50: Na+/H+ exchanger regulatory factor 1; PDZ protein: Post-synaptic density-95, disks-large and zonula occludens-1 protein; SLC9A3R1 protein: solute carrier family 9, subfamily A, member 3 regulator 1 protein; IVM: in vitro maturation; COCs: cumulus-oocyte complexes; PBS: phosphate buffered saline; FBS: fetal bovine serum; TCM-199: tissue culture medium 199; Pb: polar body; BSA: bovine serum albumin; MII: Metaphase II; CB: cytochalasin B; mSOF: modified sheep oviduct fluid; mSOFaa: modified sheep oviduct fluid supplemented with Essential and non-essential amino acids; DAPI: 4, 6-diamidino-2-phenylindole;

Declarations

Acknowledgments

We thank Song Gao and Mengyun Wang for their assistance with the laboratory techniques.

Conflict of interest

The authors declare that they have no conflicts of interest with the contents of this article.

Author contributions

Zhenzi Zuo, Yongsheng Wang, Yong Zhang, and Suzhu Qin designed the experiments. Zhenzi Zuo, Yue Du, Fang Qiao and Zheng Wang performed the experiments. Xu Liu and Jingyi Wang analyzed the results. Zhenzi Zuo wrote the paper.

Funding

This work was supported by the National Natural Science Foundation of China (No. 31972572), the National Major Project for Production of Transgenic Breeding (No. 2016ZX08007003), and the Natural Science Foundation of Shannxi Province (No. 2020JM-171)

Availability of data and materials

The datasets supporting the conclusions of this article are included within the article.

Ethics approval and consent to participate

No experimental animals were used in the present study, the bovine oocytes were collected from ovary derived from slaughter-house.

Consent for publication

Not applicable.

Competing interests

The authors declare that they have no competing interests.

References

1. Stanton J-AL, Macgregor AB, Mason C, Dameh M, Green DPL. Building comparative gene expression databases for the mouse preimplantation embryo using a pipeline approach to UniGene. *Mol Hum Reprod* 2007;13:713-720.
2. Ostermeier GC, Miller D, Huntriss JD, Diamond MP, Krawetz SA. Reproductive biology: Delivering spermatozoan RNA to the oocyte. *Nature* 2004;429:154-154.
3. Du Y, Wang X, Wang B, Chen W, Zhang Y. Deep Sequencing Analysis of microRNAs in Bovine Sperm. *Mol Reprod Dev* 2014;81:1042-1052.
4. Wang B, Wang Y, Zhang M, Du Y, Zhang Y, Xing X, Zhang L, Su J, Zhang Y, Zheng Y. MicroRNA-34c Expression in Donor Cells Influences the Early Development of Somatic Cell Nuclear Transfer Bovine Embryos. *Cellular reprogramming* 2014;16:418-427.
5. Wang M, Gao Y, Qu P, Qing S, Qiao F, Zhang Y, Mager J, Wang Y. Sperm-borne miR-449b influences cleavage, epigenetic reprogramming and apoptosis of SCNT embryos in bovine. *Sci Rep* 2017;7:13403.
6. Rajewsky N. microRNA target predictions in animals. *Nat Genet* 2006;38 Suppl:S8-13.
7. Lewis BP, Burge CB, Bartel DP. Conserved seed pairing, often flanked by adenosines, indicates that thousands of human genes are microRNA targets. *Cell* 2005;120:15-20.
8. Peter ME. Targeting of mRNAs by multiple miRNAs: the next step. *Oncogene* 2010;29:2161-2164.
9. Wang M, Gao Y, Qu P, Qing S, Qiao F, Zhang Y, Mager J, Wang Y. Sperm-borne miR-449b influences cleavage, epigenetic reprogramming and apoptosis of SCNT embryos in bovine. *Sci Rep* 2017;7:13403.
10. Lowery AJ, Miller N, Dwyer RM, Kerin MJ. Dysregulated miR-183 inhibits migration in breast cancer cells. *BMC Cancer* 2010;10:502.
11. Wang G, Mao W, Zheng S. MicroRNA-183 regulates ezrin expression in lung cancer cells. *FEBS Lett* 2008;582:3663-3668.
12. Zhao H, Guo M, Zhao G, Ma Q, Ma B, Qiu X, Fan Q. miR-183 inhibits the metastasis of osteosarcoma via downregulation of the expression of ezrin in F5M2 cells. *Int J Mol Med* 2012;30:1013-1020.

13. Sato N, Funayama N, Nagafuchi A, Yonemura S, Tsukita S, Tsukita S. A gene family consisting of ezrin, radixin and moesin. Its specific localization at actin filament/plasma membrane association sites. *J Cell Sci* 1992;103 (Pt 1):131-143.
14. Berryman M, Franck Z, Bretscher A. Ezrin is concentrated in the apical microvilli of a wide variety of epithelial cells whereas moesin is found primarily in endothelial cells. *J Cell Sci* 1993;105 (Pt 4):1025-1043.
15. Bonilha VL, Finnemann SC, Rodriguez-Boulan E. Ezrin promotes morphogenesis of apical microvilli and basal infoldings in retinal pigment epithelium. *J Cell Biol* 1999;147:1533-1548.
16. Saotome I, Curto M, McClatchey AI. Ezrin is essential for epithelial organization and villus morphogenesis in the developing intestine. *Dev Cell* 2004;6:855-864.
17. Wang HJ, Zhu JS, Zhang Q, Guo H, Dai YH, Xiong XP. RNAi-mediated silencing of ezrin gene reverses malignant behavior of human gastric cancer cell line SGC-7901. *J Dig Dis* 2009;10:258-264.
18. Zwaenepoel I, Naba A, Da Cunha MM, Del Maestro L, Formstecher E, Louvard D, Arpin M. Ezrin regulates microvillus morphogenesis by promoting distinct activities of Eps8 proteins. *Mol Biol Cell* 2012;23:1080-1094.
19. Viswanatha R, Bretscher A, Garbett D. Dynamics of ezrin and EBP50 in regulating microvilli on the apical aspect of epithelial cells. *Biochem Soc Trans* 2014;42:189-194.
20. Lange K. Fundamental role of microvilli in the main functions of differentiated cells: Outline of an universal regulating and signaling system at the cell periphery. *J Cell Physiol* 2011;226:896-927.
21. Lecce L, Lindsay LA, Murphy CR. Ezrin and EBP50 redistribute apically in rat uterine epithelial cells at the time of implantation and in response to cell contact. *Cell Tissue Res* 2011;343:445-453.
22. Wang YS, Zhao X, Su JM, An ZX, Xiong XR, Wang LJ, Liu J, Quan FS, Hua S, Zhang Y. Lowering storage temperature during ovary transport is beneficial to the developmental competence of bovine oocytes used for somatic cell nuclear transfer. *Anim Reprod Sci* 2011;124:0-54.
23. Quanli, An, Wei, Peng, Yuyao, Cheng, Zhenzhen, Lu, Chuan, Zhou. Melatonin supplementation during in vitro maturation of oocyte enhances subsequent development of bovine cloned embryos. *J Cell Physiol* 2019.
24. Qu P, Zuo Z, Liu Z, Niu Z, Zhang Y, Du Y, Ma X, Qiao F, Wang M, Zhang Y. Sperm-borne small RNA regulate α-tubulin acetylation and epigenetic modification of early bovine somatic cell nuclear transfer embryos. *Mol Hum Reprod* 2019.
25. Zhang J, Qu P, Zhou C, Liu X, Ma X, Wang M, Wang Y, Su J, Liu J, Zhang Y. microRNA-125b is a key epigenetic regulatory factor that promotes nuclear transfer reprogramming. *J Biol Chem*;292(38):jbc.M117.796771.
26. Zhu J, Feng Y, Ke Z, Zheng Y, Zhou J, Huang X, Wang LJAJoP. Down-Regulation of miR-183 Promotes Migration and Invasion of Osteosarcoma by Targeting Ezrin. *Am J Pathol* 2012;180:2440-2451.
27. Yuan S, Schuster A, Tang C, Yu T, Ortogero N, Bao J, Zheng H, Yan W. Sperm-borne miRNAs and endo-siRNAs are important for fertilization and preimplantation embryonic development.

Development (Cambridge, England) 2016;143:635-647.

28. Liu WM, Pang RT, Chiu PC, Wong BP, Lao K, Lee KF, Yeung WS. Sperm-borne microRNA-34c is required for the first cleavage division in mouse. *Proc Natl Acad Sci U S A* 2012;109:490-494.
29. Conine CC, Sun F, Song L, Rivera-Pérez JA, Rando OJ. Small RNAs Gained during Epididymal Transit of Sperm Are Essential for Embryonic Development in Mice. *Dev Cell* 2018;46:470-480.e473.
30. Zhou X, Shi X, Quan S. Transgenerational transmission mediated by small non-coding RNA in sperm. *National journal of andrology* 2016;22:1021-1024.
31. Lange K. Role of microvillar cell surfaces in the regulation of glucose uptake and organization of energy metabolism. *Am J Physiol Cell Physiol* 2002;282:C1-26.
32. Granot I, Bechor E, Barash A, Dekel N. Connexin43 in rat oocytes: developmental modulation of its phosphorylation. *Biol Reprod* 2002;66:568-573.
33. Runge KE, Evans JE, He ZY, Gupta S, McDonald KL, Stahlberg H, Primakoff P, Myles DG. Oocyte CD9 is enriched on the microvillar membrane and required for normal microvillar shape and distribution. *Dev Biol* 2007;304:317-325.
34. Garris DR. Ultrastructural aspects of the appositional stage of interstitial blastocyst implantation. *Gynecol Obstet Invest* 1984;17:10-17.
35. Blankenship TN, Given RL, Parkening TA. Blastocyst implantation in the Chinese hamster (Cricetulus griseus). *Am J Anat* 1990;187:137-157.
36. Reczek D, Berryman M, Bretscher A. Identification of EBP50: A PDZ-containing phosphoprotein that associates with members of the ezrin-radixin-moesin family. *J Cell Biol* 1997;139:169-179.
37. Weinman EJ, Steplock D, Shenolikar S. NHERF-1 uniquely transduces the cAMP signals that inhibit sodium-hydrogen exchange in mouse renal apical membranes. *FEBS Lett* 2003;536:141-144.
38. Morales FC, Takahashi Y, Kreimann EL, Georgescu MM. Ezrin-radixin-moesin (ERM)-binding phosphoprotein 50 organizes ERM proteins at the apical membrane of polarized epithelia. *Proc Natl Acad Sci U S A* 2004;101:17705-17710.
39. Garbett D, LaLonde DP, Bretscher A. The scaffolding protein EBP50 regulates microvillar assembly in a phosphorylation-dependent manner. *J Cell Biol* 2010;191:397-413.
40. Bretscher A, Chambers D, Nguyen R, Reczek D. ERM-Merlin and EBP50 protein families in plasma membrane organization and function. *Annu Rev Cell Dev Biol* 2000;16:113-143.
41. Hanono A, Garbett D, Reczek D, Chambers DN, Bretscher A. EPI64 regulates microvillar subdomains and structure. *J Cell Biol* 2006;175:803-813.
42. LaLonde DP, Garbett D, Bretscher A. A regulated complex of the scaffolding proteins PDZK1 and EBP50 with ezrin contribute to microvillar organization. *Mol Biol Cell* 2010;21:1519-1529.

Tables

Table 1. Primer sequences of target genes for PCR

Gene	Primer Sequences	Length (nt)
EZR-WT	F: CCCAATGGTATCATAGTGCC	405
	R:TGCGTAGGGAGTGCGTCAA	
Nck2-WT	F:CCATGAGCCACAGAGCAG	331
	R:CTTGAAACGAGCCGAAGG	
Ppp2a-WT	F: CTAATGGATATGGGAAGACG	503
	R:ATGAGGCTGAGATTTGAGAA	
Crk-WT	F:CCAAAAGCAAATGCAAGA	416
	R:TTCAAAAGATCACCAAGC	
Teme150a-WT	F:CCCCGCATCTCCTTTGCAT	224
	R:AAGGGCTGGCTGGGTGAAT	
Srek1ipi-WT	F:TAGTACCTGCCTCCTTCGTT	435
	R: CACTGCTCCTGAGATTTATGAC	
Pdcd6-WT	F:TAATGAAACAAGCACCAACG	411
	R:ACGGACAGGCACAAGGAT	
Map3k4-WT	F:TTCCACAAAGACCGCACC	321
	R:CGGCAGACAGGAGACTAACAG	
Slc35a1-WT	F:AAGGTTAAAGTGCCAAAGCC	388
	R:GAGAGCCCGACAGTTACATAC	

Table 2. Primer sequences of site-directed mutated target genes for PCR

Gene	Mutation Primer Sequence	Length (nt)
EZR-MUT	F:CTTATATTCTTGTAACGCCTTTTTTTCT	405
	R:AGAAAAAAAGGCGTTACAAGAATATAAG	
Nck2-MUT	F:CCCCCCCAACTGTAACGCAGCAGAGTG	331
	R:CACTCTGCTGCGTTACAGTTGGGGGGG	
Ppp2a-MUT	F:CCAAAAAGATTGTAACGCTAAAAATAC	503
	R:GTATTTTTAGCGTTACAATCTTTTTGG	
Crk-MUT	F:TATGAAACATTGTAACGTGTATTATAA	416
	R:TTATAATACACGTTACAATGTTTCATA	
Teme150a-MUT	F:CCCACACCTTGTAACGAGAGGAGCGG	224
	R:CCGCTCCTCTCGTTACAAGGTGTGGG	
Srek1ipi-MUT	F:TTTTACAAATTGTAACGCTTGGCATGTC	435
	R:GACATGCCAAGCGTTACAATTTGTAAAA	
Pdcd6-MUT	F:GCTGTTAATTTGTAACGGAGGTAACAT	411
	R:ATGTTACCTCCGTTACAAATTAACAGC	
Map3k4-MUT	F:TGCGTGCCAATGTAACGTACTACTGTA	321
	R:TACAGTAGTACGTTACATTGGCACGCA	
Slc35a1-MUT	F:TGCTGTCTTTTGTAACGTCATTGTCTGG	388
	R:CCAGACAATGACGTTACAAAAGACAGCA	

Table 3. Primer sequences for real-time-qPCR

Gene	Primer Sequences
EZR	F:GACTGCTGGGCACGCTCATA
	R:TTCTGGACGGGTTTTCTCGC
Ppp2ca	F:ACTGGTGCCATGACCGAAAT
	R:GTGCTGGGTCAAACTGCAAG
Pdcd6	F:AGCAAGCCCTCTCAGGTTTC
	R:GAAGTCGTCGAAGGCGATCT
Slc9a3r1	F: GGGATCGGTGTTTGATCCCC
	R: GTAGCCGTTCGGACCCTTC
H2a	F:GAGGAGCTGAACAAGCTGTTG
	R:TTGTGGTGGCTCTCAGTCTTC
GAPDH	F:ATCTCGCTCCTGGAAGATG
	R:TCGGAGTGAACGGATTCG

Figures

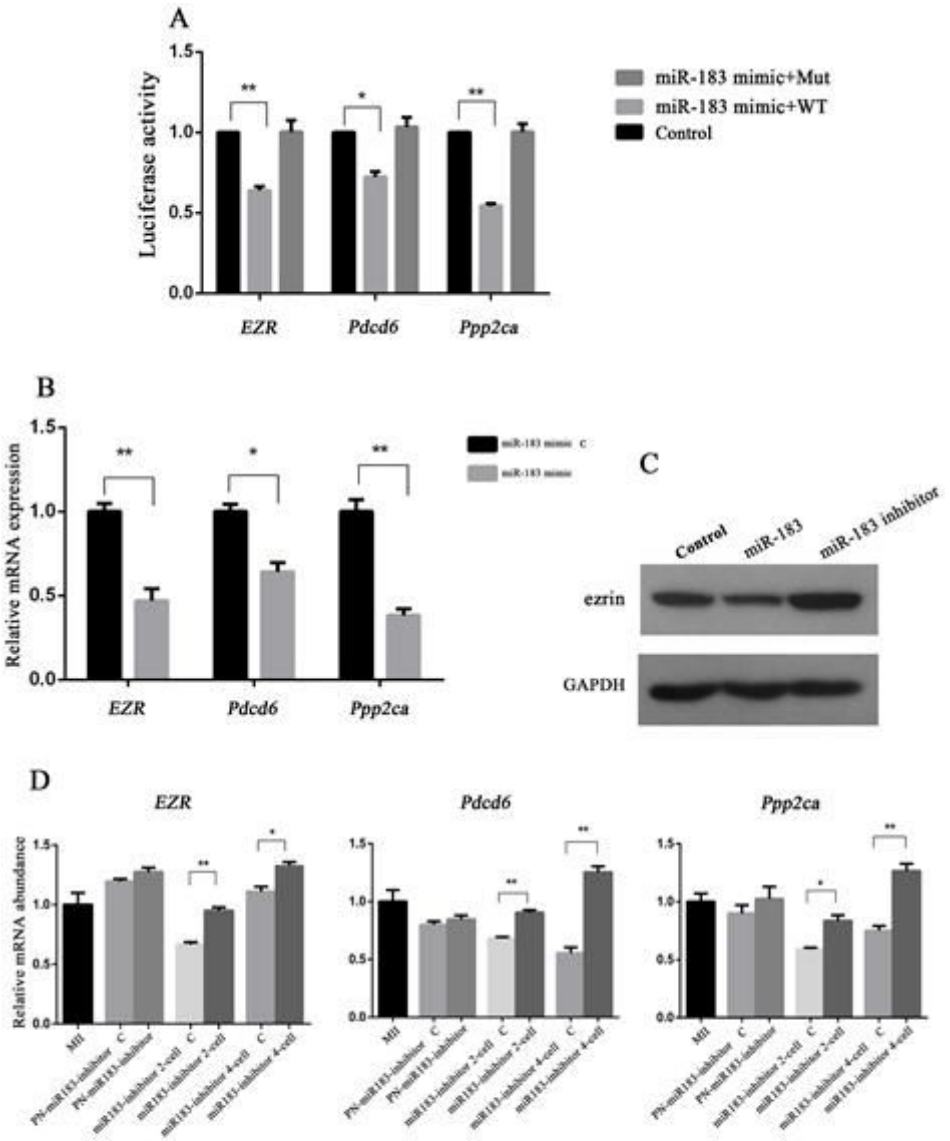

Figure 1

Screening the target genes of miRNA-183. (A) 3'UTR reagent fluorescence analysis after miR-183 treatment. Statistical comparisons were conducted by one-way ANOVA. (B) Analysis of expression levels of EZR, Pdcd6, and Ppp2ca mRNAs after miR-183 mimic or mimic control treatment by real-time PCR. (C) Protein levels of ezrin and GAPDH after miR-183 mimic transfection by western immunoblotting. (D) Expression levels of target genes of EZR, Ppp2ca and Pdcd6 in SCNT and IVF Embryos. C: mimic control. * indicates significant difference between groups ($p<0.05$), ** indicates extremely significant difference between groups ($p<0.01$).

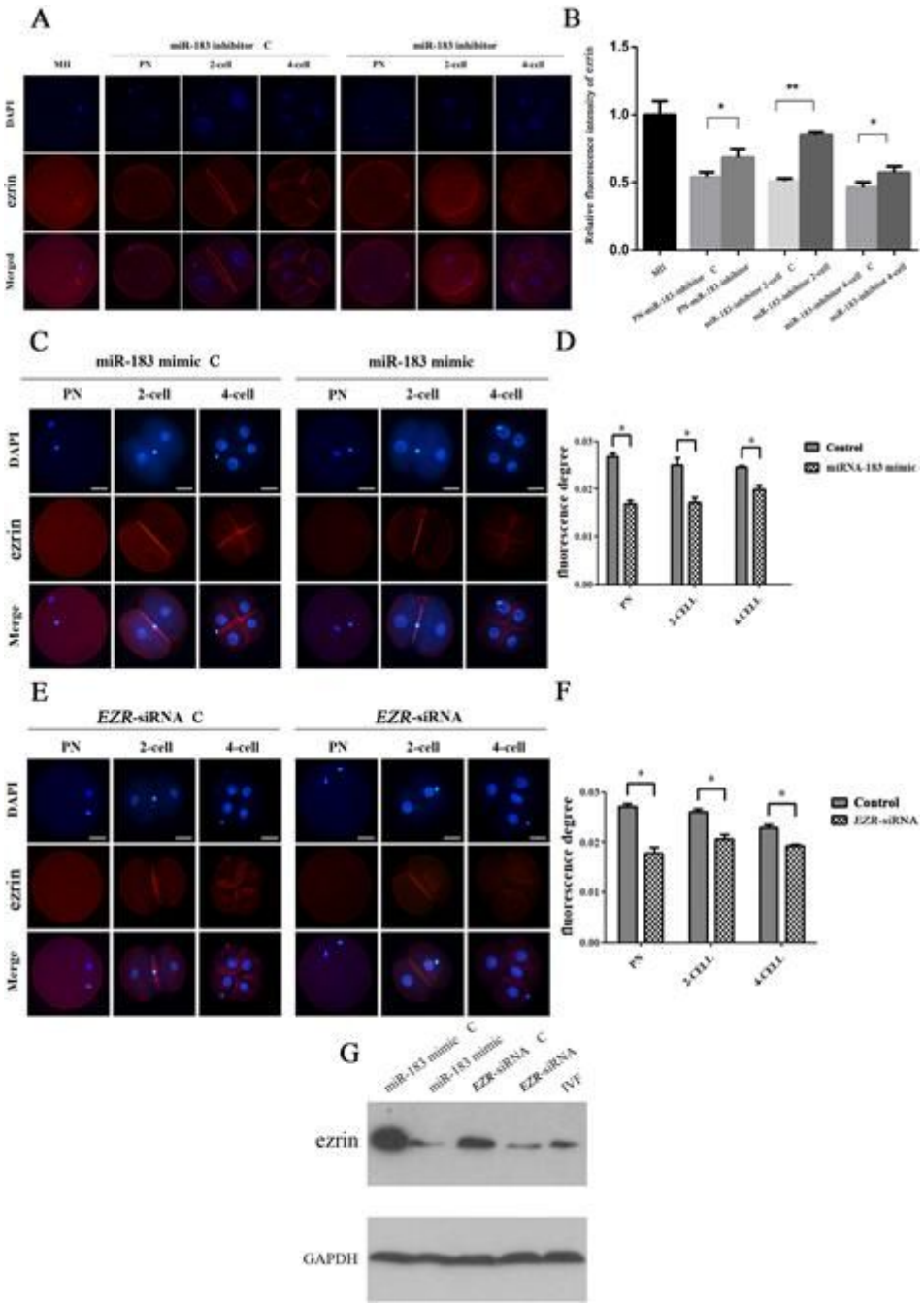

Figure 2

Verification of the targeting relationship between miR-183 and its target gene, EZR. (A) Immunofluorescence changes in expression of ezrin protein in PN, 2-cell and 4-cell stages of IVF embryos and MII oocytes after microinjection of miR-183 inhibitor and mimic control; bar = 40 μm. (B) Analysis of expression levels of ezrin protein after microinjection of miR-183 inhibitor and mimic control. * indicates significant difference between groups ($p<0.05$), ** indicates an extremely significant difference between groups ($p<0.01$. (C) Expression of ezrin protein in parthenogenetic embryos after injection of miR-183 mimic in PN, 2-cells and 4-cells. (D) * indicates significant difference between groups ($p<0.05$); bar = 40 μm. (E) Expression of ezrin protein in parthenogenetic embryos after injection of EZR-siRNA in PN, 2-cell

and 4-cell stage embryos. (F) * indicates significant difference between groups ($p<0.05$); bar = 40 μm. (G) Expression of ezrin in parthenogenetic embryos after injection of miR-183 mimic. C: mimic control.

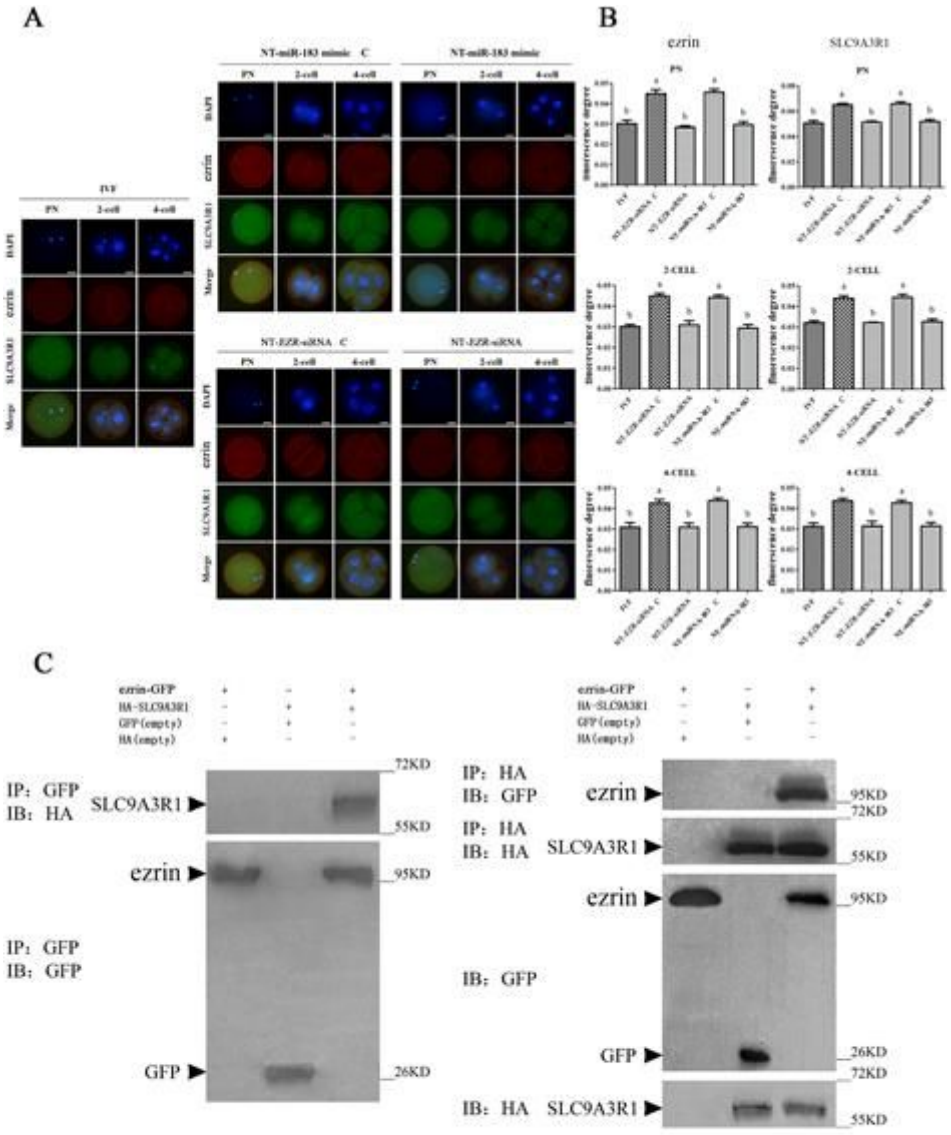

Figure 3

Screening and validation of the proteins interacting with ezrin. (A) Ezrin is mainly expressed on the surface of cell membranes, and SLC9A3R1 is highly expressed in cytoplasm. (B) Fluorescence imaging of ezrin and SLC9A3R1 expression was analyzed by Image J software at different stages of IVF embryos, NT-EZR-siRNA C, NT-EZR-siRNA, NT-miR-183 C, NT-miR-183. Different superscripts (a-b) indicate significant differences for each gene ($p<0.05$); bar = 40 μm. (C) From left to right: ezrin-GFP and HA-empty, GFP- empty and HA-SLC9A3R1, ezrin-GFP and HA-SLC9A3R1. C: mimic control.

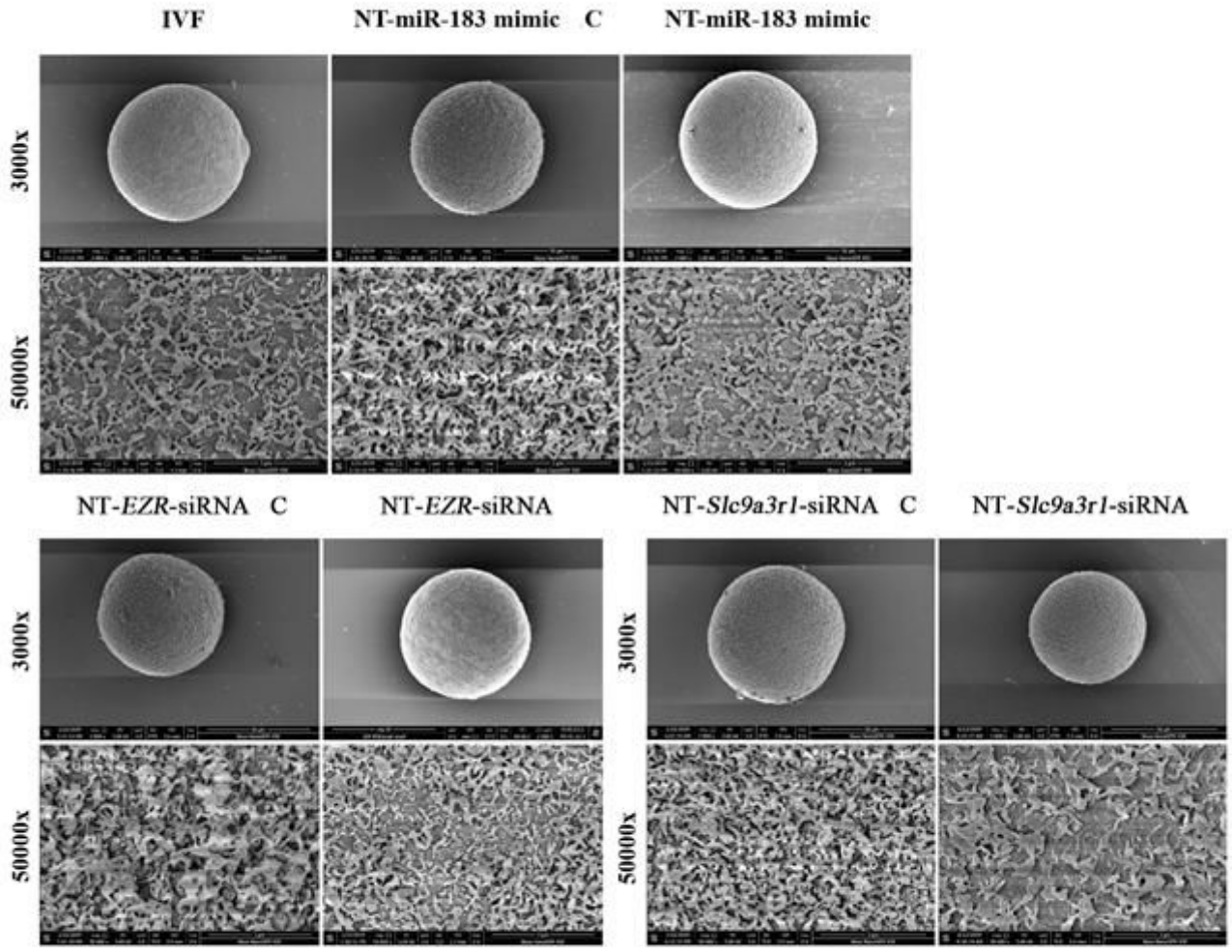

Figure 4

MiR-183 targets ezrin to regulate microvillus formation in early bovine embryos. Surface microvillus structure of IVF, NT-miR-183 mimic C, NT-miR-183 mimic, NT-EZR-siRNA C, NT-EZR-siRNA, NT-Slc9a3r1-siRNA C, and NT-Slc9a3r1-siRNA embryos. C: mimic control.

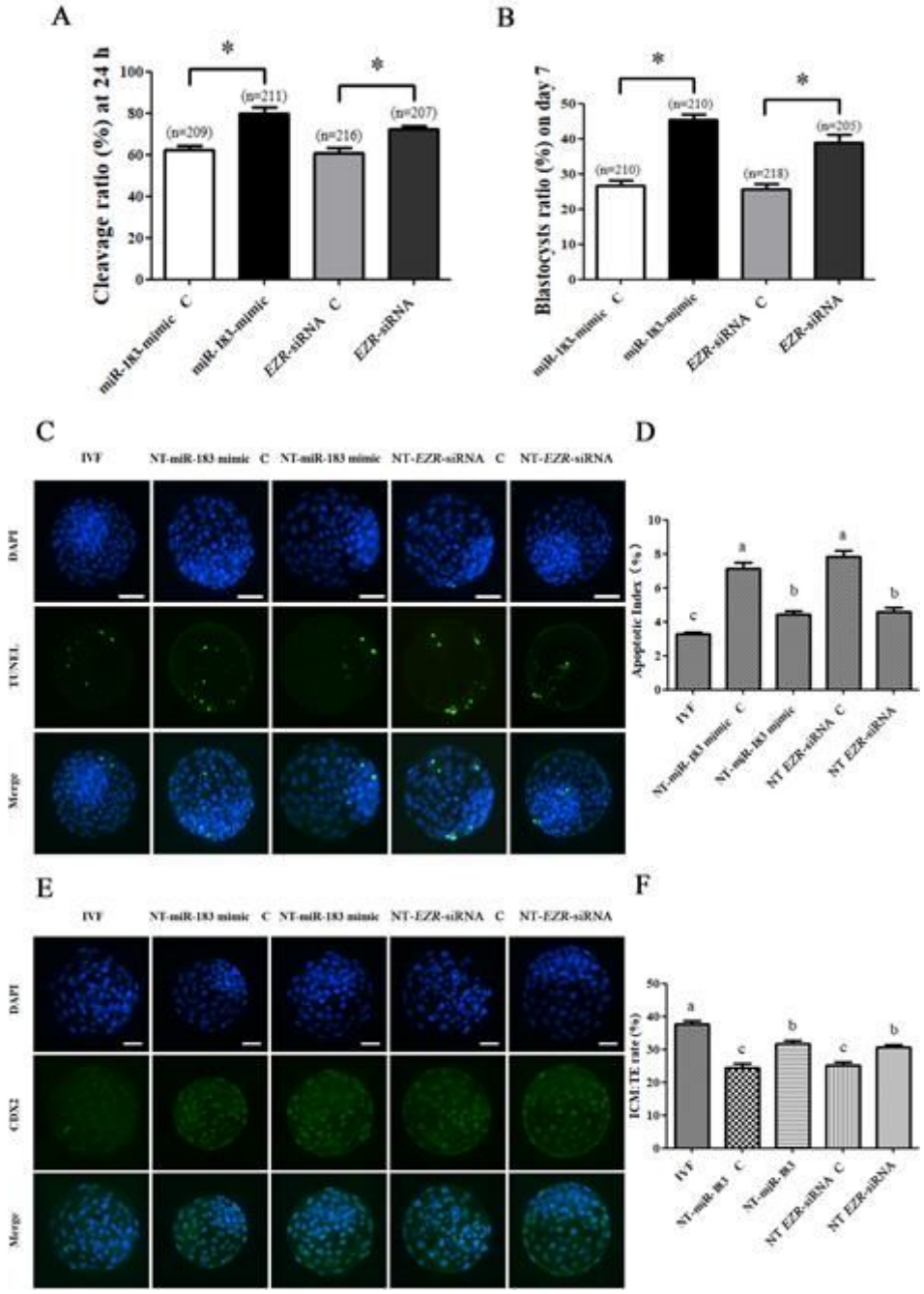

Figure 5

Effects of miR-183-ezrin on the developmental competence of bovine embryos. (A) The cleavage rate in 24 h and (B) blastocyst formation rate at day 7 of NT-miR-183 mimic C, NT-miR-183 mimic, NT-EZR-siRNA C, and NT-EZR-siRNA embryos. * indicates significant difference between groups ($p<0.05$). (C) Blastocyst apoptosis of IVF embryo, NT-miR-183 mimic C, NT-miR-183 mimic, NT-EZR-siRNA C, and NT-EZR-siRNA embryos. (D) Different superscripts (a-c) indicate significant differences for each gene ($p<0.05$); bar = 80 μm. (E) ICM: TE rate of IVF, NT-miR-183 mimic C, NT-miR-183 mimic, NT-EZR-siRNA C, and NT-EZR-siRNA embryos. (F) Different superscripts (a-c) indicate significant differences for each gene ($p<0.05$); bar = 80 μm. C: mimic control.

Supplementary Files

This is a list of supplementary files associated with this preprint. Click to download.

- sm10.docx
- sm10.docx
- sm9.docx
- sm9.docx
- sm8.docx
- sm8.docx
- sm7.docx
- sm7.docx
- sm6.tif
- sm6.tif
- sm5.tif
- sm5.tif
- sm4.tif
- sm4.tif
- sm3.tif
- sm3.tif
- sm2.tif
- sm2.tif
- sm1.tif
- sm1.tif